Discussion of "Equivalent Static Wind Loads on Buildings: New Model" by Xinzhong Chen and Ahsan Kareem

October 2004, Vol. 130, No. 10, pp. 1425–1435.
DOI: 10.1061/(ASCE)0733-9445(2004)130:10(1425)

Yin Zhou[1]
[1]Senior Engineer, Cermak Peterka Petersen, Inc., 1415 Blue Spruce Dr. #3, Fort Collins, CO 80524. E-mail: yzhou@cppwind.com

The authors proposed a rigorous model for evaluating equivalent static wind loading (ESWL) on tall buildings as a linear combination of mean, background, and resonant components. In this model, the mean and resonant ESWL components are essentially the same as those reported in such literature as Zhou et al. (2000) and Zhou and Kareem (2001). However, the treatment of background ESWL (BESWL) introduced some improvements.

The BESWL in the conventional displacement-based gust loading factor (GLF) model (Davenport 1967; Zhou et al. 1999), as used in most current codes and standards, and that in a newly developed bending-moment-based GLF model (Zhou and Kareem 2001) produce accurate estimates for limited wind load effects only, such as the first model displacement or base bending moment, while providing approximate estimates for others. Unlike those "approximate" models, the proposed BESWL will induces the exact wind load effect of interest. In contrast with a previous "accurate" ESWL model (Holmes 2002a,b), which also involves a linear combination of wind load components while the distribution of its BESWL varies for different wind effects, the proposed model uses a unique background loading pattern, the gust loading envelope, which offers some convenience for the purpose of design application.

Nonetheless, the discusser would like to raise two concerns associated with the proposed ESWL model.

1. By definition, the ESWL is a wind force and when it is applied statically, the response found by static analysis is equivalent to the response through more detailed stochastic study. Taking the background component as an example, the BESWL is a load that can satisfy the following equation

$$\int_0^H F_{eR_b}(z) \cdot \mu_x(z) dz = R_{b\,\max} \tag{1}$$

where $R_{b\,\max} = g_b \cdot \sigma_{R_b}$ is the peak background wind load effect associated with the influence function $\mu_x(z)$. In other words, any load pattern that can satisfy Eq. (1) provides a solution for the BESWL. The number of solutions is numerous.

Apparently, the proposed BESWL in Eq. (7) of the paper is one of many solutions found by substituting Eqs. (7) and (8) of the original paper into Eq. (1) of this discussion. Similarly, one can suggest a different BESWL with a different distribution pattern, such as that proposed by Holmes (2002a,b). In various models, the loading pattern could have different physical implications.

In addition to those two loading patterns, two formats of BESWL may interest design engineers. The first is a loading following the mean wind force, which is expressed in a format that is similar to Eq. (7) of the original paper

$$F_{eR_b}(z) = B_z \cdot B_{\bar{P}} \cdot \bar{P}_x(z) \tag{2}$$

$$B_{\bar{P}} = \frac{\int_0^H F'_{ebx}(z) \cdot \mu_x(z) dz}{\int_0^H \bar{P}_x(z) \cdot \mu_x(z) dz} = \frac{g_b \cdot \sigma'_{R_b}}{\bar{R}} \tag{3}$$

Another is a loading pattern following the resonant ESWL

$$F_{eR_b}(z) = B_z \cdot B_{F_{er}} \cdot F_{erx}(z) \tag{4}$$

$$B_{F_{er}} = \frac{\int_0^H F'_{ebx}(z) \cdot \mu_x(z) dz}{\int_0^H F_{erx}(z) \cdot \mu_x(z) dz} \tag{5}$$

In Eqs. (2)–(4), $B_{\bar{P}}$ and $B_{F_{er}}$ are adjustment factors. Both Eqs. (2) and (4) satisfy Eq. (1). The mean-wind-force distributed BESWL in Eq. (2) is easier for design engineers to understand. The inertial-force-type BESWL in Eq. (4) has the same distribution as the resonant ESWL; therefore, those two components can be arithmetically combined and Eq. (10) of the original paper can be simplified.

2. As previously mentioned, the proposed ESWL model, along with another "accurate" model (Holmes 2002a,b), can produce an accurate estimate for the wind load effect associated with the influence function $\mu_x(z)$. However, this outcome does not occur without a cost.

The ESWL in Eq. (10) of the original paper was developed for any particular wind response involving several factors, such as the background factor B_z and the combination factors, which vary for different wind load effects under consideration. Therefore, for a different wind load effect, a different ESWL will be needed. For the wind-resistant design of a particular structure, the wind load effects that are of concern to the design engineers are numerous, e.g., the internal forces in all structural members. To provide accurate design of all structural members, a large number of combined ESWL, will be needed in the design process. Furthermore, in principle, by using any one of these ESWLs in the structural analysis, the design engineer can only obtain the accurate estimate of the wind load effect corresponding to the influence function that was employed in developing the ESWL. In fact, this wind load effect is already available before the ESWL can be given in Eq. (10) of the paper.

A possible way to employ the "accurate" ESWL model in a real design practice is to find several generic loading patterns, if they exist, from a large pool of ESWLs by using the proposed procedure, which will lead to accurate estimates for some wind load effects while providing reasonably good estimates for others. Unless these loading patterns do exist and the number of loading

patterns needed is within a feasible range, the potential application of the proposed model is substantially limited for any real design or code practice.

References

Davenport, A. G. (1967). "Gust loading factors." *J. Struct. Div. ASCE*, 93(1), 11–34.

Holmes, J. D. (2002a). "Gust loading factor to dynamic response factor (1967-2002)." *Symp. Preprints, Engineering, Symp. to Honor Alan G. Davenport for his 40 years of contributions*, Univ. of Western Ontario, London, Ontario, Canada, A1-1-A1-8.

Holmes, J. D. (2002b). "Effective static load distributions in wind engineering." *J. Wind. Eng. Ind. Aerodyn.*, 90, 91–109.

Zhou, Y., Gu, M., and Xiang, H. F. (1999). "Along-wind static equivalent wind loads and response of tall buildings. I: Unfavorable distributions of static equivalent wind loads." *J. Wind. Eng. Ind. Aerodyn.*, 79(1–2), 135–150.

Zhou, Y., Kareem, A., and Gu, M. (2000). "Equivalent static buffeting loads on structures." *J. Struct. Eng.*, 126(8), 989–992.

Zhou, Y., and Kareem, A. (2001). "Gust loading factor: New model." *J. Struct. Eng.*, 127(2), 168–175.

Closure to "Equivalent Static Wind Loads on Buildings: New Model" by Xinzhong Chen and Ahsan Kareem

October 2004, Vol. 130, No. 10, pp. 1425–1435.
DOI: 10.1061/(ASCE)0733-9445(2004)130:10(1425)

Xinzhong Chen[1] and Ahsan Kareem[2]

[1]Assistant Professor, Wind Science and Engineering Research Center, Dept. of Civil Engineering, Texas Tech Univ., Lubbock, TX 79409. E-mail: xinzhong.chen@ttu.edu

[2]Robert M. Moran Professor, NatHaz Modeling Laboratory, Dept. of Civil and Geological Sciences, Univ. of Notre Dame, Notre Dame, IN 46556. E-mail: kareem@nd.edu

The authors would like to thank the discusser for the discussion and interest in this important topic that concerns immediate design applications and that is not clearly understood by some in the research community. Our response to this discussion also gives us an opportunity to further clarify and highlight the background, motivation, and contributions of our work on the modeling of equivalent static wind loads (ESWLs) on buildings.

The modeling of ESWLs seeks static load distributions whose static effects on buildings are equivalent to the actual dynamic wind-load effects. This load representation allows designers to follow a relatively simple static analysis procedure for predicting building response to spatiotemporally varying dynamic loads. This approach is often more suitable for design practice because of its simplicity and expedience. This format serves as a pivotal piece of information for estimating response under the combined action of wind and other loads and is widely used in current building codes and standards worldwide.

For a given peak response, a variety of ESWL distributions may be defined on the basis of different considerations. The load distribution is not necessarily unique simply because different load distributions may result in identical building response. The major challenge in developing an equivalent load representation for a given building lies in seeking distributions that are physically meaningful and that are insensitive to individual response. Consequently, the number of loading distributions for a variety of important response components may be limited (Chen and Kareem 2005).

One approach for extracting the equivalent loading is the gust loading factor (GLF), or gust response factor (GRF), approach, which has been widely used in major building codes and standards around the world (Davenport 1967). In this scheme, the equivalent wind loading used for design is equal to the mean wind load multiplied by a GRF, which is customarily based on the displacement at the top of the building. The GRF is defined as the ratio of peak dynamic response to its mean value. Although the traditional GRF approach is simple to use in the building design process, the GRF may vary widely for different response components of a structure and may have significantly different values for structures with similar geometric configurations but different structural systems. As illustrated in Chen and Kareem (2004), among others, for the along-wind response of buildings, the GRFs for the top displacement and base bending moment are almost the same and are generally larger than that for the base shear force. The GRF for the building response at higher elevations is generally markedly larger than that for the top displacement or base bending moment. Therefore, the equivalent loading given by the mean load multiplied by the GRF for the top displacement or base bending moment generally leads to underestimating building response at higher elevations. Furthermore, the GRF approach cannot be extended to the across-wind and torsional responses, which are typically characterized by low values of mean wind loading and associated response, particularly for symmetric buildings.

The dynamic response factor (DRF) approach is another way of modeling equivalent loading and has been adopted in some building codes. The DRF has been defined as the ratio of peak dynamic response (including the mean, background, and resonant components) to the response caused by the peak dynamic load that includes the mean and background load effects but excludes any reduction attributable to loss of spatial correlation of wind loading. The DRF for a given response can be related to its GRF and the background factor (Chen and Kareem 2005). The background factor represents the reduction effect with respect to the background (quasi-static) response attributable to loss of spatial correlation of wind loading. The DRF approach results in an equivalent load distribution that is similar to the peak dynamic load (including the mean) scaled by the DRF. Compared with the GRF approach, the advantage of the DRF approach is that it can be applied not only to the along-wind component but also to the across-wind and torsional response components. The disadvantage is that the DRF may vary markedly for different response components, particularly for dynamically sensitive tall buildings.

Separating the ESWLs into background and resonant components provides a physically more meaningful description of loading. It is straightforward to express the resonant ESWL (RESWL) as the inertial load in the fundamental mode, which depends on the mass distribution and mode shape. The advantage of this load description over the traditional GRF approach is that it leads to a universal load distribution for all resonant response components. Within the traditional GRF approach, different GRFs and associated loads have to be assigned for accurate predictions of distinct response components. This advantage is attributable to the presumption that the primary contributor to the resonant response is the fundamental mode and that the higher mode contributions are negligible. This load distribution is also consistent with the seis-

mic loading provided in current building codes and standards worldwide.

Compared with the straightforwardness of RESWL, modeling the background ESWL (BESWL) is relatively complex. This complexity is attributed to the nature of partially correlated multiple inputs of wind loading. Under the action of dynamic loading, different background response components generally reach their peaks at different times. When the BESWL for a given peak background response is directly derived from the conditional sampling and subsequent ensemble average of dynamic pressures over the building surface at the instant when the desired peak load effect occurs, the load distribution varies with the individual response under consideration (e.g., Tamura et al. 2003). The ensemble average of this conditional sampling of dynamic pressures is very close to the load distribution provided by using the load-response-correlation (LRC) approach (Kasperski 1992), which results in a most probable load distribution for a given peak response. According to the LRC approach, each response component corresponds to a distinct spatial load distribution. This feature may limit its potential application to design standards or practice. To eliminate the dependence of load distribution on individual response, an approximate model of the BESWL has been suggested in Holmes (1996). This scheme provided an identical load distribution for any building response at the same building elevation, but the response components at different elevations have distinct load distributions.

A universal load distribution for all background response components has been suggested in Katsumura et al. (2004) with application to a large-span cantilever roof. According to this scheme, the BESWL for any peak background response is expressed as a linear combination of the loading modes with larger eigenvalues, which are derived through proper orthogonal decomposition of the loading covariance matrix. The combination factors are independent of individual response and are determined in a least square sense for better estimations of selected important response components.

As the discusser points out and as used in the literature, the BESWL can be expressed in terms of the mean load multiplied by background GRF (BGRF), similar to the traditional GRF approach for the total response. As illustrated in Chen and Kareem (2004), the BGRF varies for a wide range for different response components. Obviously, this approach will suffer the same disadvantages as the traditional GRF approach. The BESWL given in terms of the inertial load of the fundamental mode is less accurate for background response because the higher mode contributions to the background response cannot simply be ignored.

Taking the aforementioned information as the background and motivation, our study attempted to develop an advanced model of the wind loading on buildings that could be applied to low-, middle-, and high-rise buildings. In the proposed framework, the ESWLs for the background and resonant response components were developed separately, with a new model, called the gust loading envelope (GLE), for modeling the BESWL. This approach results in a load distribution similar to the gust loading envelope but scaled by a background factor. The background factor depends on individual response. For a global response, the background factor is much less than unity; whereas for a local response, it may be close to unity. The background factor is potentially insensitive to the individual response; therefore, simplification of equivalent loading may be achieved. Another advantage of this approach is that it can be applied not only to the along-wind component but also to the acrosswind and torsional response components. It can also be applied to transient wind load effects on buildings. The difference of this approach from the DRF approach is also very clear. The proposed GLE approach is used to model the BESWL, whereas the DRF approach is for the total ESWL, including the mean, background, and resonant components.

After the BESWL and RESWL have been determined for a given peak response, the corresponding peak background and resonant response components are calculated by following a static analysis procedure. They are then combined for the total peak response (excluding the mean component) by using the square root of the sum of squares (SRSS) approach. Alternatively, the ESWL for the total peak response can be determined with a direct combination of the background and resonant loading by using a linear combination scheme, as discussed in Chen and Kareem 2004. The combination factors or weighting factors depend on individual response, specifically on the response ratio of the background and resonant components. By examining the ESWLs for a variety of important response components of a given building, the number of equivalent load distributions could be significantly limited. The goal of this study is to develop advanced modeling of equivalent load distributions that are physically meaningful, potentially insensitive to individual response, and therefore easy for applications with a limited number of loadings for all important building response components. This advanced modeling also facilitates interpolating or extrapolating wind loads between buildings and terrains.

The last issue that the writers would like to address is related to the application of the ESWL modeling. The discusser seems to raise a question by the statement "In fact, this wind load effect is already available before the ESWL can be given in Eq. (10)"; that is why the ESWL is needed, since we already know the response. Like every approach for modeling equivalent loading, including the GRF approach, dynamic response analysis must be carried out during the process of developing the equivalent loading to make sure that the equivalent loading can result in the same or a slightly conservative response as compared with the peak dynamic wind load effect. The resulting equivalent loading is not used to quantify the wind load effect that we already know but is used for other response components of the same building or those of similar buildings.

References

Chen, X., and Kareem, A. (2004). "Equivalent static wind loads on buildings: New model." *J. Struct. Eng.*, 130(10), 1425–1435.

Chen, X., and Kareem, A. (2005). "Evaluation of equivalent static wind loads on buildings." *Proc., 10th Americas Conference on Wind Engineering* (CD-ROM), American Association for Wind Engineering, Baton Rouge, La.

Davenport, A. G. (1967). "Gust loading factors." *J. Struct. Div. ASCE*, 93(1), 11–34.

Holmes, J. D. (1996). "Along-wind of lattice towers: Part III. Effective load distribution." *Eng. Struct.*, 18, 483–488.

Kasperski, M. (1992). "Extreme wind load distributions for linear and nonlinear design." *Eng. Struct.*, 14, 27–34.

Katsumura, A., Tamura, Y., Nakamura, O., and Yoshida, T. (2004). "Universal equivalent static wind load distribution on a large span cantilevered roof." *Proc., 18th National Symp. on Wind Engineering*, Japan Association for Wind Engineering, Tokyo, 461–466.

Tamura, Y., Kikuchi, H., and Hibi, K. (2003a). "Quasi-static wind load combinations for low- and middle-rise buildings." *J. Wind. Eng. Ind. Aerodyn.*, 91(12–15), 1613–1625.

Discussion of "Influence of Foundation Flexibility on R_μ and C_μ Factors" by Javier Avilés and Luis Eduardo Pérez-Rocha

February 2005, Vol. 131, No. 2, pp. 221–230.
DOI: 10.1061/(ASCE)0733-9445(2005)131:2(221)

Mohammad Ali Ghannad[1] and Hossein Jahankhah[2]
[1]Assistant Professor, Dept. of Civil Engineering, Sharif Univ. of Technology, P.O. Box 11365-9313, Tehran, Islamic Republic of Iran. E-mail: ghannad@sharif.edu
[2]Ph.D. Student, Dept. of Civil Engineering, Sharif Univ. of Technology, P.O. Box 11365-9313, Tehran, Islamic Republic of Iran. E-mail: jahan807@yahoo.com

The paper concludes that "the real values of $R_{\mu-\beta}$ for short structures are practically the same as those of $R_{\mu-\infty}$. In contrast, they are notably lower for tall structures." This conclusion was reached by comparing the results of Fig. 9 for soil-structure systems with those of Fig. 5 for the fixed-base state. In the other words, the authors concluded that the soil-structure interaction (SSI) effect on $R_{\mu-\beta}$ is negligible for squatty buildings with $H_e/r=1$ and can be dominant for slender buildings such as when $H_e/r=5$. However, the conclusion does not seem to be correct, since all parts of the graphs shown in Fig. 9 are not meaningful for conventional building-type structures. The authors refer to the same point in relation to the results of Fig. 7 for the case of $H_e/r=3$. In considering a typical case with constant system parameters, the authors calculate an effective height of around 37.5 m, which corresponds to a building of approximately 15 stories. In explaining the results of Fig. 7, they correctly state that "the discrepancies observed at short natural periods are not of practical significance, since midrise structures such as the one studied normally fall in the medium-period spectral range. For a 15-story building, T_e may vary between, say, 1.1 and 1.8 s, depending on the structural system." Following the same method, the effective height of buildings with $H_e/r=1$ and $H_e/r=5$ would be about 12.5 and 62.5 m, which corresponds to buildings of approximately 5 and 25 stories, respectively. Consequently, for example, for the case of $H_e/r=1$, T_e may vary in the range of, say, 0.3 to 0.8 s and not more. Comparing the results of Fig. 9 and Fig. 5 in this range reveals that the SSI effect is not negligible for conventional squatty buildings. For more clarification, the next paragraph studies the subject systematically.

The nondimensional frequency $\eta=\omega r/\beta_s$ is an index for the importance of the SSI effect in soil-structure systems. Therefore, looking at this value for each case is necessary before making any conclusion. The authors use the natural frequency of the system to calculate this parameter. For the sake of simplicity, consider η_{fix} as a new nondimensional frequency that is calculated on the basis of the natural period of the fixed-base structure. The period of any soil-structure system is in all circumstances longer than the period of the fixed-base structure, i.e., $\eta > \eta_{fix}$. We next study the practical range of this parameter for conventional cases. As a rule of thumb, the period of building-type structures can be approximated as $T_e=0.1\times N$, in which N=number of stories and T_e=period of structure in seconds. Considering an interstory height of 3.5 m and an effective heights of 0.7 times the total height, the result is the following formula for η_{fix}

$$\eta_{fix}=50\pi r/H_e\beta_s \tag{1}$$

The practical range of this parameter is therefore not the same for buildings with different aspect ratios. A new parameter can be defined as the product of η_{fix} and H_e/r, as follows

$$\hat{\eta}_{fix}=50\pi/\beta_s \tag{2}$$

This parameter can be used as a global index for the severity of the SSI effect regardless of the aspect ratio of the building. Considering an extremely low shear-wave velocity of $\beta_s=50$ m/s leads to an upper limit of π for $\hat{\eta}_{fix}$, so $\hat{\eta}_{fix}$ ranges from zero, which is indeed the fixed-base state, to almost 3, where the SSI effect is dominant. The SSI plays no important role when η_{fix} is less than 1 (Ghannad et al. 1998). We next examine the results presented in the paper from this point of view. With the fixed values of $r=12.5$ m and $\beta_s=76$ m/s, η_{fix} will be a function of only the period of structure, i.e., $\eta_{fix}=1.0/T_e$. Accordingly, $\hat{\eta}_{fix}=(1.0/T_e)\cdot H_e/r$. For the model used by the authors the SSI effect decreases rapidly as the period of the structure increases, especially for squatty buildings. For example, for $H_e/r=1$, no significant SSI effect exists even for the period of 1 s, and the model almost behaves as fixed-base for longer periods. Indeed, the results of Fig. 9 is very similar to the results of Fig. 5 for periods longer than 1 s for this reason. In contrast, for $H_e/r=5$, $\hat{\eta}_{fix}$ is larger than 1 for the entire period range shown in Fig. 9 and reaches the value of 2.5 for a period of 2 s, which is expected for a 25-story building. Therefore, comparing the results of Fig. 9 for $H_e/r=1$ and $H_e/r=5$ in the present form is not as meaningful. Thus, the general conclusion for the effect of the SSI on the strength reduction factor of short and tall buildings is not valid. In fact, the paper leaves a false impression that for squatty buildings with $H_e/r=1$ (which is not necessarily a short building in general) located on soft soils, one may use the same strength reduction factors computed for the fixed-base model. The research of the discussers (Ghannad and Jahankhah 2004) show that this result is not correct and that using this idea leads to large ductility demands in the designed structure.

References

Ghannad, M. A., Fukuwa, N., and Nishizaka, R. (1998). "A study on the frequency and damping of soil-structure systems using a simplified model." *J. Struct. Eng.*, Architectural Institute of Japan (AIJ), 44B, 85–93.

Ghannad, M. A., and Jahankhah, H. (2004). "Strength reduction factors considering soil-structure interaction." *Proc. 13th World Conf. on Earthquake Engineering (13WCEE)* (CD-ROM) Vancouver, Canada.

Discussion of "Influence of Foundation Flexibility on R_μ and C_μ Factors" by Javier Avilés and Luis Eduardo Pérez-Rocha

February 2005, Vol. 131, No. 2, pp. 221–230.
DOI: 10.1061/(ASCE)0733-9445(2005)131:2(221)

Chad Harden, M.ASCE[1]; and
Tara Hutchinson, M.ASCE[2]

[1]Design Engineer, RBF Consulting, 14725 Alton Parkway, Irvine, CA. E-mail: charden@rbf.com

[2]Assistant Professor, Dept. of Civil and Environmental Engineering, Univ. of California, Irvine, CA 92697-2175. E-mail: thutchin@uci.edu

The paper presents an excellent examination of the effects of including soil flexibility in superstructure design. Study and recommendations on this topic are greatly needed by the design community. In fact, the question is not whether to include soil flexibility (and perhaps nonlinearity), since *not* including the effects of soil flexibility may be *unconservative* for displacement-sensitive structural components. In addition to the effects of soil flexibility, the results of which are well presented in this paper, foundation uplift is a nonlinear behavior that may influence design of the superstructure. Foundation uplift is a reasonable expectation for moderately compliant soils and especially for design-level seismic demands imposed on high vertical factor of safety shallow-foundation-supported structures. The authors did not explore this concept, therefore it is considered in this discussion in order to extend the treatment presented in the paper. Comparison with current design code recommendations, using an isolated case with and without foundation uplift, is considered in this discussion to call attention to the practical importance of these effects on design displacement demands (Harden et al. 2005, 2006).

In this discussion, a linear elastic system is described as an elastic rigid-column element (i.e., shearwall) resting on an elastic Winkler subgrade. Nonlinearity is introduced by allowing a second identical system to uplift through a gap in the Winkler springs. In this way, the effect of foundation uplift on structural displacement demands was isolated independent of soil hysteresis and superstructure ductility. To present the results in a format that follows current design recommendations, such as FEMA 356 (2000) and ATC-40 (1996), the point of incipient uplift is prescribed for specific force reduction R-values, and the resulting displacement modification factor C_1 (ratio of maximum displacement of the nonlinear (uplifting) system to the elastic system) is calculated for a number of time-history analyses. Time histories are computed by using the longitudinal component of a suite of 19 unscaled time histories described by Somerville and Collins (2002). These motions represent a broad range of peak ground accelerations (0.13 to 0.75 g), peak ground velocities (9.1 to 84.8 cm/s) and peak ground displacements (1.2 to 18.7 cm) levels. Simulations were performed in the OpenSEES platform (PEER 2005).

Comparing the maximum displacements of the nonlinear system with the elastic system resulted in a recommended value for C_1 as presented in Eq. (1), which is based on binning and regressing the data with respect to the specified force reduction factor and the ratio of the maximum acceleration of the two systems:

$$C_1 = \frac{1}{1 + Ae^{-B(T/T_S - 0.5)}} \tag{1}$$

where A and B are regressed coefficients; and the ratio T/T_S is the ratio of the elastic period of the system to the characteristic period of the ground motion (determined by using a Newmark-Hall spectrum (Newmark and Hall 1987). Results from this study for an elastic system allowed to uplift can easily be incorporated into the authors' formulation with a few simplifications to Eq. (17), repeated here:

$$R_{\mu-\beta} = 1 + (\tilde{\mu}_e - 1)\frac{\tilde{T}_e}{T_e}\left(\frac{\tilde{U}_m(\tilde{T}_e, \tilde{\zeta}_e)}{U_g}\right)^{\alpha} \tag{2}$$

Consider, for example, the response of an elastic system of a shallow foundation not allowed to uplift with natural period T_e, compared with that of a nonlinear elastic system of a shallow foundation allowed to uplift with natural period $\tilde{T}_e$. In this case, the ratio $\tilde{T}_e/T_e \equiv 1$ before uplift, since the only nonlinear contribution to the system is through uplift. Additionally, for an elastic superstructure ($\mu_e = 1$), the total system ductility $\tilde{\mu}_e = C_1$.

Since displacement of the uplifting system may not be known, consider converting the spectral displacement demands to

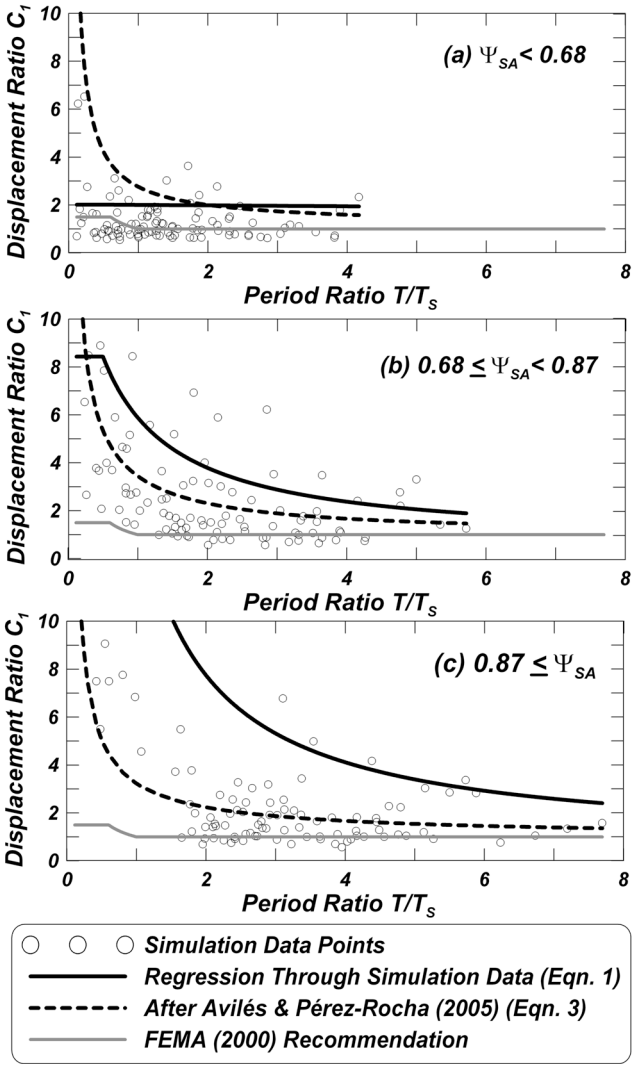

Fig. 1. Binned data—C_1 versus normalized period for $R = 4.0$

acceleration demands, such that the ratio $\tilde{U}_m(\tilde{T}_e, \tilde{\zeta}_e)/U_g \equiv (\omega_g^2/\omega_n^2)(A_m/A_g)$. With these simplifications, Eq. (2) reduces to

$$R = 1 + (C_1 - 1)\left(\frac{T_n^2}{T_S^2}\frac{A_m}{A_g}\right)^{\alpha} \quad (3)$$

where T_S=characteristic period of the ground motion. The theoretical value of C_1 is calculated from Eq. (3) for a constant value of R=4.0 and is compared with the results presented in Harden et al. (2006), as shown in Fig. 1. Although Eq. (3) is not as sensitive to the ratio of acceleration of the nonlinear to elastic system, abbreviated as the variable ψ_{SA}, in general, a conservative estimate of C_1 is found. For example, for the binned case of $\psi_{SA} < 0.87$, approximately 72% of the time-history results fall below the curve represented by Eq. (3). In addition, two approaches—one based on time-history analyses, the other based on a theoretical solution—yield similar trends. These two approaches result in a good comparison for period ratios above approximately 1.0, leading to the conclusion that uplifting foundation effects will be most influential on displacement demands at low period ratios (less than 1.0) and higher normalized acceleration values ψ_{SA}. Given the additional number of time histories performed for this discussion (the study of the original paper, compared with only one ground motion time history analysis), it is reasonable to conclude that ground motion effects, duration, and frequency all affect the shape and amplitude of the C_1-R-T/T_s relations.

References

Applied Technology Council (ATC). (1996). "Seismic evaluation and retrofit of concrete buildings." *ATC-40*, Vols. 1 and 2, Redwood City, Calif.

Federal Emergency Management Agency (FEMA). (2000). "Prestandard and commentary for the seismic rehabilitation of buildings." *FEMA Publication 356*, prepared by the American Society of Civil Engineers for the Federal Emergency Management Agency, Washington, D.C.

Harden, C. W., Hutchinson, T. C., Kutter, B. L., and Martin, G. R. (2005). "Numerical modeling of the nonlinear cyclic response of shallow foundations." *Technical Report 2005/04*, Pacific Earthquake Engineering Research (PEER) Center, Univ. of California, Berkeley, Calif.

Harden, C., Hutchinson, T. C., and Moore, M. (2006). "Investigation into the effects of foundation uplift on simplified seismic design procedures." *Earthquake Spectra*, in press.

Newmark, N., and Hall, W. (1987). *Earthquake spectra and design*, EERI Monograph Series, Earthquake Engineering Research Institute, Oakland, Calif.

Pacific Earthquake Engineering Research Center (PEER). (2005). *OpenSEES: Open system for earthquake engineering simulation platform*, University of California, Berkeley, ⟨http://opensees.berkeley.edu/⟩ (Jan. 2005).

Somerville, P., and Collins, N. (2002). "Ground motion time histories for the Van Nuys Building." PEER Methodology Testbeds Project, http://www.peertestbeds.net/van%20nuys.htm (Jan. 2004).

Closure to "Influence of Foundation Flexibility on R_μ and C_μ Factors" by Javier Avilés and Luis Eduardo Pérez-Rocha

February 2005, Vol. 131, No. 2, pp. 221–230.
DOI: 10.1061/(ASCE)0733-9445(2005)131:2(221)

Javier Avilés[1] and Luis Eduardo Pérez-Rocha[2]

[1]Researcher, Instituto Mexicano de Tecnología del Agua, Paseo Cuauhnahuac 8532, Jiutepec 62550, Morelos, Mexico. E-mail: javiles@tlaloc.imta.mx

[2]Researcher, Instituto de Investigaciones Eléctricas, Paseo de la Reforma 113, Temixco 62490, Morelos, Mexico. E-mail: lepr@iie.org.mx

The writers thank the discussers for their interest in the paper. We would like to comment on the following two issues that they raised:

The Effect of Slenderness

The discussers believe that the reader should be cautioned against generalizing the observations made from comparing the results of Fig. 9 for H_e/r=1 and 5. The writers agree with this remark regarding the effect of slenderness on $R_{\mu-\beta}$ factors. Such results, however, were intended only to verify the writers' approximate reduction rule given by Eq. (17) for both squat (H_e/r=1) and slender (H_e/r=5) structures. In effect, these results are not realistic over the whole interval of natural periods, because structures with H_e/r=1 normally fall in the short-period spectral region and structures with H_e/r=5 fall in the long-period spectral region. Out of each region, the goal is only to show the trend of results. Two indexes are generally used for measuring the importance of soil-structure interaction (SSI), namely, the relative stiffness of the structure and soil, $\sigma = H_e/T_e\beta_s$, and the wave transit time, $r/\beta_s = \sigma T_e r/H_e$. Since the $R_{\mu-\beta}$ factors in Fig. 9 are for fixed values of H_e/r and r/β_s ($r \approx 12.5$ m and β_s=76 m/s), the resulting σ is a decreasing function of T_e. As the discussers say, the SSI effects decrease as the natural period increases, especially for squat structures. For evaluating the effect of slenderness, presenting results for fixed values of σ is more instructive than presenting results for fixed values of r/β_s. If T_e is proportional to H_e, as happens with many building-type structures, then σ measures purely the soil flexibility.

For a representative interstory height of 3.5 m and by assuming the effective height as 0.7 of the total height and the fixed-base period as 0.1 s of the number of stories, we have $H_e/T_e \approx 25$ m/s and hence $\sigma \approx 1/3$ for β_s=76 m/s. With this result and the values used in the paper for the remaining system parameters, the normalized strength spectra for the SCT recording of the 1985 Michoacan earthquake take the shapes shown in Figs. 1 and 2 for H_e/r=1 and 5, respectively. In each figure, the results for both elastic (μ_e=1) and inelastic (μ_e=4) behavior are compared with those corresponding to the fixed-base case. For this SSI representation, the foundation radius is not constant. It varies

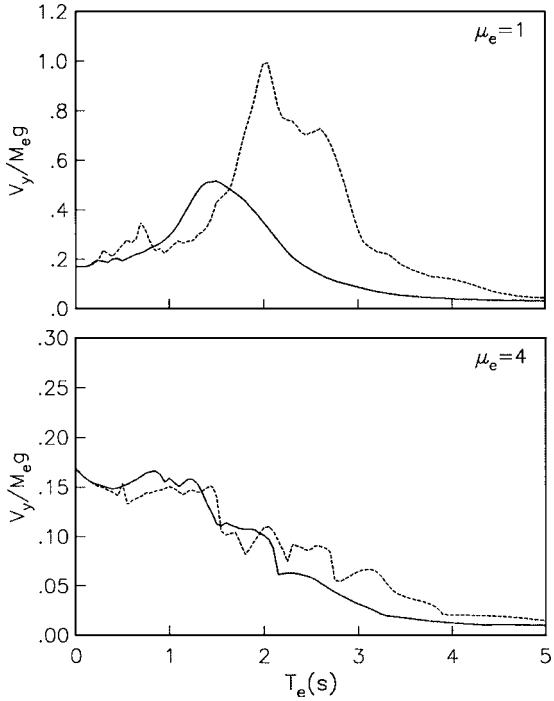

Fig. 1. Comparison between normalized strength spectra with (solid line) and without (dashed line) SSI effects for slenderness ratio $H_e/r=1$, considering $\sigma=1/3$ for relative stiffness of structure and soil

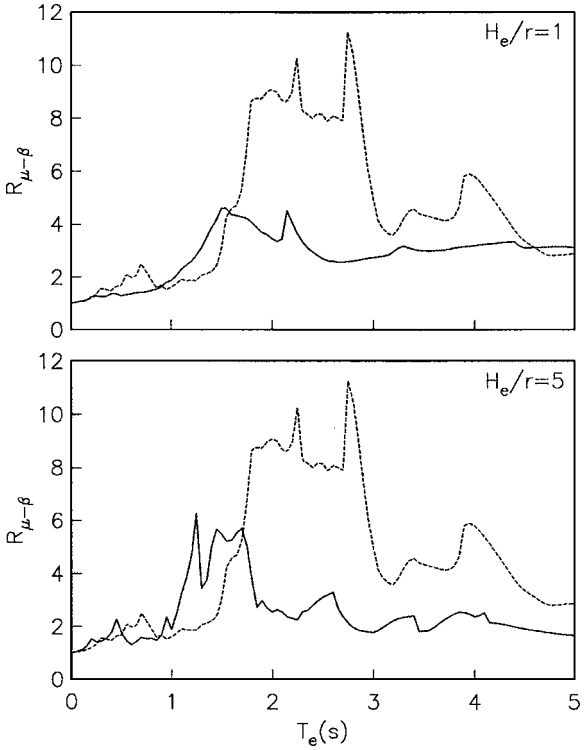

Fig. 3. Comparison between strength-reduction factors with (solid line) and without (dashed line) SSI effects for ductility factor $\mu_e=4$, considering $\sigma=1/3$ for relative stiffness of structure and soil

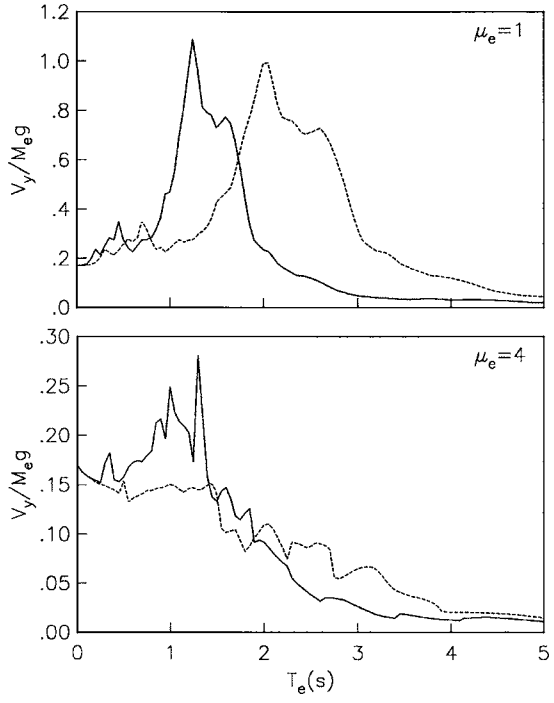

Fig. 2. Comparison between normalized strength spectra with (solid line) and without (dashed line) SSI effects for slenderness ratio $H_e/r=5$, considering $\sigma=1/3$ for relative stiffness of structure and soil

when the structure height changes, so that a fixed value of H_e/r is maintained over the entire period range. Consequently, the effect of slenderness is not exactly that of structure height. As happens with the fixed-base case, the spectral acceleration for very short period tends to the peak ground acceleration, regardless of the value of ductility. The reason for this result is that the short-period ordinates of these plots are associated with low values of r/β_s, for which the SSI effects are negligible. This outcome is especially true for slender structures. These results indicate that, for systems having the same σ, the SSI effects are equally important for squat and for slender structures, and the tendencies observed are similar in the two cases.

Strength-reduction factors are next computed by using the results of Figs. 1 and 2. The shapes of these factors with and without SSI are compared in Fig. 3 for the two slenderness ratios. In general, $R_{\mu-\beta}>R_{\mu-\infty}$ for $T_e<T_s$, except around the second mode of vibration of the soil ($\approx T_s/3$), whereas $R_{\mu-\beta}<R_{\mu-\infty}$ for $T_e>T_s$. With this SSI representation, the strength-reduction factor for very long period tends to the effective ductility, $\tilde{\mu}_e=1+(\mu_e-1)(T_e/\tilde{T}_e)^2$, which is smaller for the taller structures, where the ratio $\tilde{T}_e/T_e$ is much larger than unity. These results to some extent modify the published conclusions regarding the effect of slenderness. The differences between the $R_{\mu-\beta}$ factors for $H_e/r=1$ and $H_e/r=5$ do not show a clear tendency indicating the case that is most influenced by SSI. By following the same SSI representation, Avilés and Pérez-Rocha (2005) have evaluated the effect of slenderness on the design base shear specified by code. They have shown that SSI has the effect of increasing (for $T_e<T_s$) or decreasing (for $T_e>T_s$) the base shear with respect to the fixed-base value, with these modifications being greater for the more slender structures. Furthermore, the increments in the base shear are less important than the reductions.

The Effect of Foundation Uplift

The discussers point out that the effect of foundation uplift has not been explored in the paper and propose a simple way to account for it on the structural displacement demands. Specifically, the writers' approximate reduction rule given by Eq. (17) has been adjusted as a function of few significant parameters. However, the writers do not understand how the resulting Eq. (3) can be used for different slenderness ratios controlling the realization of rocking motion. This influence is perhaps reflected in the peak structural acceleration, A_m, for the value of which we do not have information. It is a simple matter to show that, under static conditions, the minimum ground acceleration required to initiate uplifting of a rigid structure of width $2r$ is $A_g^o/g=2r/3H_e$, whereas that needed for overturning is $A_g^u/g=2r/H_e$. The slenderness ratio is clearly a direct measure of the uplifting potential of the foundation, in addition to the peak ground acceleration. Both quantities should be reflected in any design procedure for estimating structural displacements that originate from foundation uplift.

Indeed, Makris and Konstantinidis (2003) have questioned the concept of estimating lateral displacements of rocking structures by using conventional response spectra. They have shown fundamental differences between the deformation and rocking spectra. In particular, the rocking spectra are very sensitive to the value of slenderness. Furthermore, the current design approach (FEMA 2000) has been shown by these authors to be conceptually imperfect and it should therefore be abandoned. Although the discussers' formulation is based on response spectra, it yields surprisingly good predictions of the structural displacement demands. The writers do not have a clear answer to this finding, which may be attributable to accidental similarities between the deformation and rocking spectra. We can only say that the nonlinear SSI effects associated with structure yielding and foundation uplifting are two radically different phenomena, so the solution of one problem may not be directly applicable to the solution of the other. Further research in this direction is required.

References

Avilés, J., and Pérez-Rocha, L. E. (2005). "Design concepts for yielding structures on flexible foundation." *Eng. Struct.*, 27(3), 443–454.

FEMA. (2000). "Prestandard and commentary for the seismic rehabilitation of buildings." *FEMA Publication 356*, prepared by the American Society of Civil Engineers for the Federal Emergency Management Agency, Washington, D.C.

Makris, N., and Konstantinidis, D. (2003). "The rocking spectrum and the limitations of practical design methodologies." *Earthquake Eng. Struct. Dyn.*, 32, 265–289.